MEASUREMENTS OF THE SPECTRA AND AVERAGE NUMBER OF NEUTRONS EMITTED IN THE FISSION OF U^{235} AND U^{238} INDUCED BY 14.3-Mev NEUTRONS

Yu. A. VASIL' EV, Yu. S. ZAMYATNIN, Yu. I. IL' IN, E. I. SIROTININ, P. V. TOROPOV, and É. F. FOMUSHKIN

Submitted to JETP editor August 5, 1959

J. Exptl. Theoret. Phys. (U.S.S.R.) **38**, 671-684 (March, 1960)

The fission neutron spectra and average number of neutrons $\bar{\nu}$ emitted in the fission of U^{235} and U^{238} induced by 14.3-Mev neutrons were measured. The measurements were made at energies between 0.4 and 5 Mev by the time-of-flight technique, in which a pulsed source was used. The spectra obtained are interpreted as consisting of neutrons emitted by the fragments and of neutrons evaporated before fission of the nucleus. The following distribution parameters were found: $T_f = (1.06 \pm 0.03)$ Mev, $T = (0.37 \pm 0.04)$ Mev and α, the fraction of the evaporated neutrons, $= (16 \pm 2)\%$ for U^{235}; whereas $T_f = (1.16 \pm 0.03)$ Mev, $T = (0.4 \pm 0.04)$ Mev, $\alpha = (21 \pm 2)\%$ for U^{238}. The measured values of $\bar{\nu}$ are 4.17 ± 0.30 for U^{235} and 4.28 ± 0.30 for U^{238}, their ratio being $\bar{\nu}(U^{238})/\bar{\nu}(U^{235}) = 1.03 \pm 0.03$.

1. INTRODUCTION

MOST investigations into the various aspects of nuclear fission have been devoted to the study of nuclear fission by thermal neutrons and spontaneous fission. The study of nuclear fission by fast neutrons, especially the spectra and number of neutrons emitted, has been much more meager. This situation is largely due to the experimental difficulties inherent in recording fission neutrons in a background of many primary neutrons having approximately the same energy, as well as to the considerably smaller fission cross section for fast neutrons.

However, good reasons exist for the study of nuclear fission by fast neutrons: e.g., the occurrence of new fission channels at high excitation energies and the increase in the number of available fissionable isotopes.

At the present time data are available on the spectra of fission neutrons from the fission of U^{233}, U^{235}, Pu^{239}, and Pu^{241} induced by thermal neutrons[1-6] and from the spontaneous fission of Cf^{252}.[6] These measurements indicate that the spectra for all these isotopes are similar and can be approximated accurately enough by the expression

$$F(E) \sim \exp\left(-\frac{E}{T_f}\right) \sinh \frac{2\sqrt{wE}}{T_f} \qquad (1)$$

or

$$F(E) \sim \sqrt{E} e^{-E/B}. \qquad (2)$$

A slight hardening of the spectrum is noted in the transition from U^{235} to Pu^{239} and on to Cf^{252}. At present, because of insufficient experimental data, it is difficult to say whether the parameter Z^2/A plays a decisive role in this hardening.

Only the work of Zamyatnin et al.[7] contains data on the neutron spectrum for nuclear fission induced by neutrons with an energy of more than 1 Mev. In this work the photographic technique was used to study the fission neutron spectrum formed by the capture of 14-Mev neutrons by Th^{232}, U^{233}, U^{235}, U^{238}, and Pu^{239} nuclei.

The results of this study combined with computations by Bat' and Kudrin[8] give evidence of a slight hardening of the spectra with an increase in the primary neutron energy, though the data remain as yet insufficient for quantitative conclusions. Besides, the experimental setup described by Zamyatnin et al.[7] is such that it is impossible to distinguish the fission neutrons from neutrons emitted in the process of inelastic scattering and the (n, 2n) reaction.

Recently several papers[9-13] have been published on $\bar{\nu}$ measurements for the fission of various isotopes by 14-Mev neutrons. However, the results obtained lack satisfactory agreement among themselves and fail to provide a basis for conclusions as to variation of $\bar{\nu}$ from isotope to isotope.

This article describes an investigation undertaken to obtain additional data on the spectra and number of emitted neutrons from the fission of U^{235} and U^{238} induced by 14.3-Mev neutrons.

II. EXPERIMENTAL TECHNIQUE AND MEASUREMENT

Experimental arrangement. Figure 1 shows the layout of the experimental apparatus.

The time-of-flight technique was used in the measurements. An essential feature of this technique was the use of a pulsed primary neutron source.

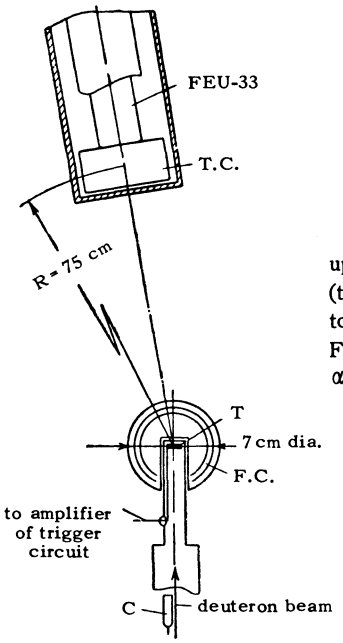

FIG. 1. Experimental setup; shaded area – Pb shield, (thickness = 2.5 mm), T.C. – tolane crystal, T – target, F.C. – fission chamber, C – α particle counter.

The primary neutron pulses were provided by a $T(d, n)He^4$ reaction in the target of the accelerator tube when the target was bombarded by short, periodic pulses of 150-kev deuterons. A fission chamber situated near the target served as the source of the fission neutrons. Since the fission incidents in the chamber occurred practically simultaneously with the primary neutron pulses, the target and the chamber constituted a pulsed source of primary and fission neutrons. Because the probability of fission inside the chamber was 10^{-4} per neutron pulse, most of the source pulses belonged to "background" and consisted of 14.3-Mev neutrons and neutrons formed by the inelastic interaction of these primary neutrons with the target materials and the fission chamber. If fission occurred in the chamber, fission neutrons likewise appeared in the source pulse. The presence of these "working" pulses was revealed by the appearance of ionization pulses in the fission chamber.

Pulses resulting from the deuteron beam bombarding the target were used as trigger pulses and determined the moment of emission of the neutrons from the source.

The neutron detector was a scintillation counter located 75 cm from the source. The time of flight of the neutrons was determined by measuring the time interval between the detector pulse and trigger pulse with an electronic circuit. The time distribution of the detector pulses was measured separately for "working" and "background" source pulses. If the total number of primary neutrons during a period of measurement was the same in the "working" and "background" source pulses, the difference in the measurements represented the time-of-flight distribution of fission neutrons. This distribution, when measured by a detector with a known energy sensitivity curve, permits one to determine the energy spectra of the fission neutrons, as well as average number of fission neutrons $\bar{\nu}$.

Pulsed source of 14.3-Mev neutrons. The pulsed deuteron flux was obtained by modulating a beam of accelerated deuterons with a sinusoidal electric field by the use of deflecting plates (f = 2 Mcs). The deuteron pulses and, correspondingly, the pulses of 14.3-Mev neutrons lasted 3 nanoseconds, and had a repetition rate of 4 Mcs. The average number of neutrons in a pulse, $\bar{n}$, was 4 (in fact $\bar{n} \approx \bar{\nu}$); any increase in the neutron yield was undesirable on account of the increase in the background. The average neutron emission was determined from the counting rate of the α monitor.

In intervals between pulses when deuterons struck the deflecting plates and the diaphragm, which was situated 80 cm from the target, 2.5-Mev neutrons were generated by the $D(d, n)He^3$ reaction. This resulted in a slight increase in background.

Fission chamber. Two fission chambers with layers of U^{235} (90%) and U^{238} (natural isotopic composition) were used. Each chamber consisted of three spheres 6, 7, and 8 cm in diameter and had a radial cylindrical channel 22 mm in diameter. The chamber electrodes and walls of the accelerator target block were constructed thin enough (0.5 mm) to reduce neutron scattering.

Layers of a fissionable substance were applied to both surfaces of the 7 mm diameter sphere. The layers in the U^{235} chamber were 2 mg/cm^2 thick and in the U^{238} chamber 3 mg/cm^2, with a thickness variation nowhere exceeding ±10%. The total weight of the fissionable substance was 0.6 g in the U^{235} chamber and 0.9 g in the U^{238} chamber. The detection efficiency of both chambers was about 60%.

The chambers were filled with a mixture of argon and carbon dioxide (10%) to a pressure of 760 mm Hg. The rise time of the chamber was $0.1 \pm 0.05\,\mu$sec.

The accelerator target was installed at the center of the chamber when spectra were being obtained. The spherically symmetrical arrangement of the fissionable substance in relation to the target eliminated the influence of anisotropy of fragment distribution on the measurements.

Neutron detector. The neutron detector was a tolane crystal, 80 mm in diameter and 25 mm thick, with a FEU-33 photomultiplier. This detector was set at a 15° angle to the axis of the accelerator tube. This placement of the detector made it possible to reduce the background due to the 2.5- Mev neutrons. The scintillation counter was sheathed in a lead shield 2.5 mm thick to protect it from x-rays from the accelerator tube.

The measurements were made in a room large enough to allow the detector to be installed no nearer than 4 m from the walls and floor and with the nearest scattering material (steel flooring 5 mm thick) 1.5 m away. Nevertheless, neutrons and γ rays that had been scattered in the room composed about half of the background in the 0.4 — 5 Mev range.

The efficiency of the detector for neutrons in the energy interval < 5 Mev was determined by Hardy's[14] method. Figure 2 shows computations for three threshold values, E_{th} (0.2, 0.25, and 0.3 Mev). To establish the energy threshold of the scintillation counter its absolute efficiency in the 0.2 — 1.5 Mev energy region was measured with an electrostatic accelerator. The T(p, n)He^3 reaction served as a source. A "long" counter and a U^{235} fission chamber were used as neutron flux monitors. Since the energy dependence of the counter efficiency for the 0.25 Mev threshold was in best agreement with the data obtained with the accelerator, this dependence was used in processing the measurements of the neutron spectra.

Electronic instrumentation. Electronic apparatus was used to measure the time distribution of the detector pulses which originated after the occurrence of working pulses from the pulsed source (i.e., after "effect + background" pulses). For our experimental conditions the time of flight for fission neutrons with energies in the 5 — 0.4 Mev region was 24 to 86 nanosec. This determined the minimum time-interval to be measured. In order to obtain data on prompt-fission γ rays and on the detector background, the time intervals measured were increased to 220 nanosec (150 nanosec after the working pulses and 70 nanosec before the pulses).

Figure 3 is a block diagram of the electronic apparatus. The system consisted of two channels — one slow, the other fast. In the slow channel, from the sequence of detector pulses those that happened to be in the interval being measured were selected; the time distribution of these pulses was measured in the fast channel. Coincidences in the slow channel were used to select the detector pulses. First, the trigger pulses that corresponded to working pulses were selected from the sequence of trigger pulses. For this purpose the trigger pulses, as well as shaped fission chamber pulses, which lasted 0.1 μsec, were fed into the slow gating circuit. With delay 1 properly selected, only working trigger pulses passed through the gating circuit; these then entered the coincidence unit with the detector pulses. If coincidence occurred, the fast gating circuit opened, and a time analyzer measured the time distribution of the corresponding detector pulses in the fast channel.

Thus, the fast channel measures the time distribution of only those detector pulses that had been produced within the exact time interval before or after the working pulses from the source. Moreover, the duration of the interval was determined by the resolution time of the coincidence circuit (220 nanosec), while the position of the interval in relation to the working trigger pulses was determined by the selection of delay 2. The interval position was maintained to within ±20 nanosec in the course of the measurements. The operation of the system is illustrated in the time diagram Fig. 4. The passage of the trigger pulses through the slow gating circuit is shown in the

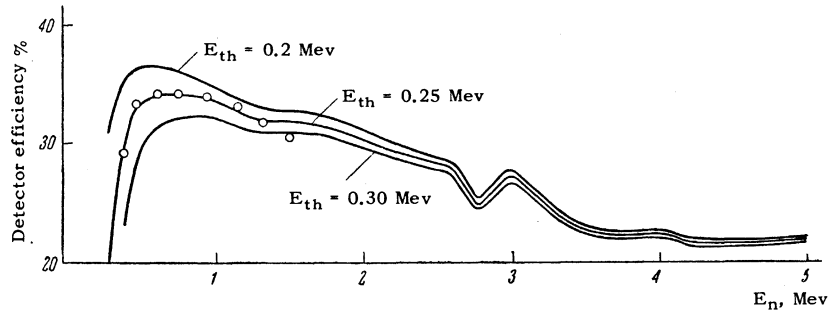

FIG. 2. Energy dependence of the detector efficiency; measurements with the electrostatic accelerator are designated by o.

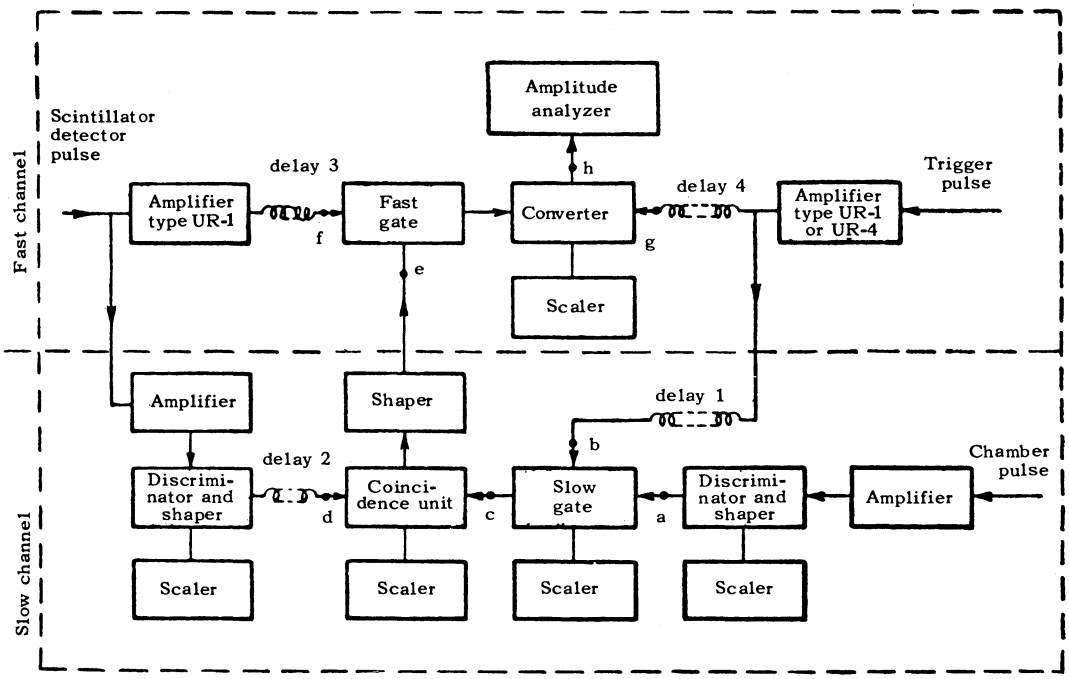

FIG. 3. Block diagram of the electronic apparatus.

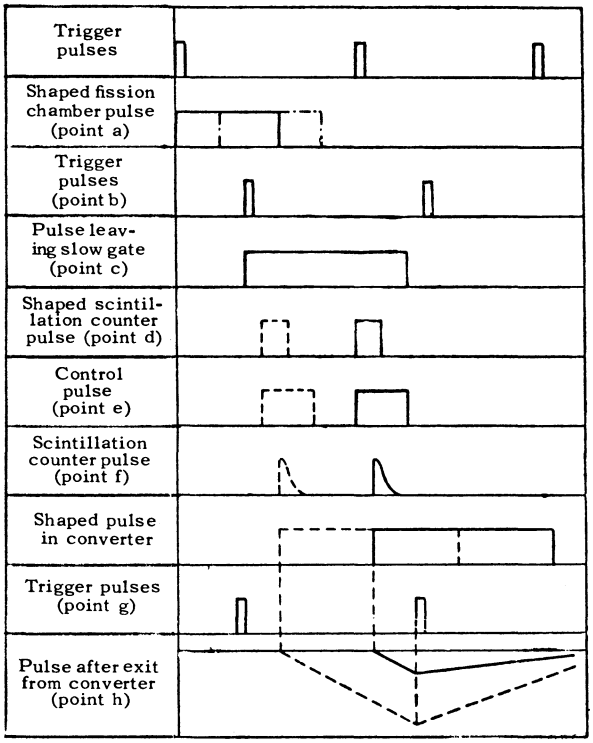

FIG. 4. Time diagram of pulses.

upper four lines. (On the second line from the top the position of the shaped fission chamber pulse is indicated during a measurement in the working interval; the dash-dot line indicates the maximum displacement of the pulse due to the scatter in the chamber rise time.) On the lower lines are the recorded detector pulses in the slow and fast channels, as well as the conversion of the time intervals between the detector and trigger pulses into an amplitude distribution. The solid and dotted lines show the pulses produced during the recording of neutrons with different times of flight.

The time distribution of the detector pulses was measured both after working source pulses (in working intervals) and after background pulses (in background intervals, which also lasted 220 nanosec). When the distribution in the background intervals was being measured, accelerator pulses instead of fission chamber pulses were admitted to the slow gating circuit. In this case, mostly background, randomly selected trigger pulses entered the coincidence circuit; the probability of transmitting working trigger pulses did not exceed 10^{-4}. The number of intervals recorded in these series of measurements was determined by the counting rate of the trigger pulses that entered the coincidence circuit (when the measurements were being made in the working intervals, the rates at which the trigger and fission chamber pulses were counted coincided).

The time analyzer used in the system operated on the principle of converting "time into amplitude." The amplitude distribution from the convertor (the input circuit of the analyzer) was measured by a 100-channel amplitude analyzer built along the lines of the ADA-50 analyzer. The average width of the time analyzer channel in the interval for recording fission neutrons and γ rays was 2.2 nanosec, and the non-linearity of the time scale did not exceed $\pm 2\%$.

Data. Figure 5 (curve a) shows the time-interval distribution of the detector pulses ob-

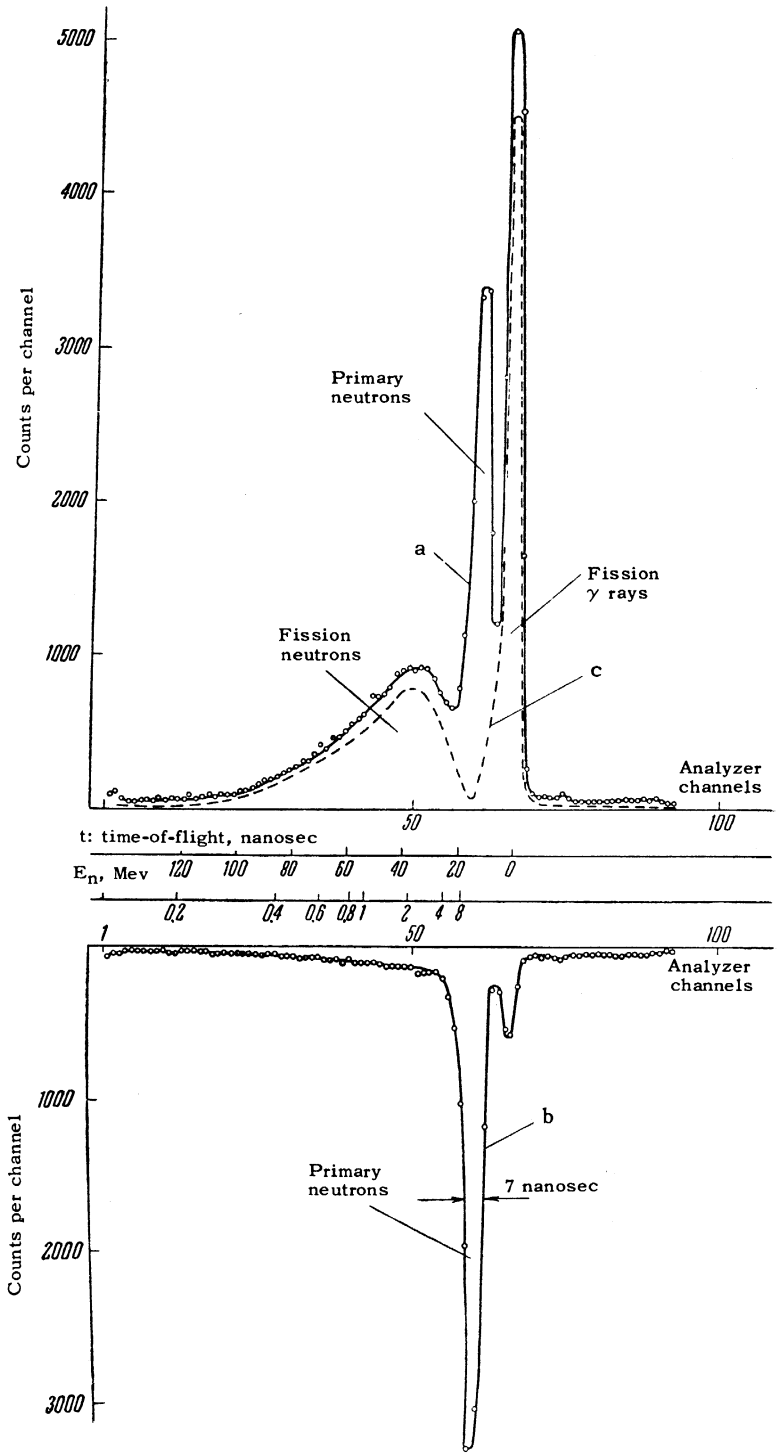

FIG. 5. Time-interval distribution of detector pulses obtained for the spectrum of neutrons from U^{238} fission; a – distribution of pulses in the working intervals, b – distribution of pulses in the background intervals, c – difference of curves a and b: time distribution of fission neutrons and γ rays.

tained in one of the series of measurements of the spectrum of neutrons emitted in U^{238} fission. On this graph one can see distinctly separate lines for the fission γ rays and 14-Mev neutrons; the broad maximum to the left corresponds to the fission neutrons.

In addition to the fission neutrons and γ rays in the working intervals, the following radiations were recorded: a) primary 14-Mev neutrons, as well as neutrons and γ rays formed in the interaction between the primary neutrons and the materials of the accelerator target block and the fission chamber; b) radiation due to the activation of materials, mostly of the scintillation counter, by fast primary neutrons; c) neutrons and γ rays formed by primary neutron scattering in the room; d) 2.5-Mev neutrons from the accelerator tube. The 14-Mev primary neutrons were separated from the fission neutrons by their time of flight. However, the other radiations enumerated above

created a background even in the region where fission neutrons were recorded.

Background data were obtained by measuring the time distribution of detector pulses in the background intervals. The procedure for measuring the spectra thus consisted of the consecutive measurements of pulse distributions in the working and background intervals. The average yield of 14.3-Mev neutrons was checked during these measurements by the counting rate of the α monitor and was maintained constant to within $\pm 3\%$. This insured the same conditions for recording background radiations in the working and background intervals.

When the distribution of detector pulses in the working intervals was being measured, background radiations a) and partly c) were proportional to $\bar{n}_w$, while radiations b) and partly c) were proportional to $\bar{n}_b$ ($\bar{n}_w$ and $\bar{n}_b$ represent the average number of primary neutrons in the working and background pulses respectively). When the distribution in the background intervals was being measured, all background radiations a), b), and c) were proportional to $\bar{n}_b$. Therefore, the method chosen for measuring the background might have led to serious error, if $\bar{n}_w \neq \bar{n}_b$. However, computations showed that $\bar{n}_w = \bar{n}_b$. In these computations it was assumed that the number of primary neutrons in the source pulses was subject to Poisson's distribution, and both the dependence of fission probability on the number of neutrons in the pulse and the capture of primary neutrons by the fissioning nucleus were taken into account.

Thus, the conditions for recording radiations a), b), and c) were the same in the working and background intervals. The accuracy of the background measurements was sufficiently high in this case, since the counting rate for uncontrolled background sources (2.5-Mev neutrons and characteristic detector noise) constituted less than 5% of the total background counting rate.

The measurements of the distributions in the working and background intervals gave rise to an equal number of recorded intervals. Figure 5 shows the frequency-time distribution of detector pulses in the background intervals that was obtained in one and the same set of measurements of the fission neutron spectrum for U^{238} (curve b). Figure 5 also shows the time distribution of neutrons and γ rays from U^{238} fission (curve c). As can be seen from the graph, the background amounted to 15 — 20% of the effect over a wide energy interval and at the limits of the 0.4 — 5 Mev energy interval amounted to 35%. This same graph shows the time and energy scales, with the zero time of the time-of-flight scale determined by the position of the fission γ-ray line. The time resolution of the apparatus as found from the half width of the fission γ-ray and primary-neutron line was 7 nanosec.

Corrections for fission neutrons scattered by the chamber and also for delayed fission γ rays[15] were applied to the data. The scattering of fission neutrons by detector materials, particularly by the lead shield, was shown by control measurements to have no effect on the spectrum measurements. Under the conditions of the experiment, measurements indicated that the effect of neutron scattering in the room could also be ignored. To illustrate the effect of the corrections Fig. 6 shows curve c (from Fig. 5) on an enlarged scale. (The shaded area corresponds to the corrections, which were subtracted during the processing of the measurements.)

To obtain the energy spectra of the fission neutrons use was made of the measurements of the

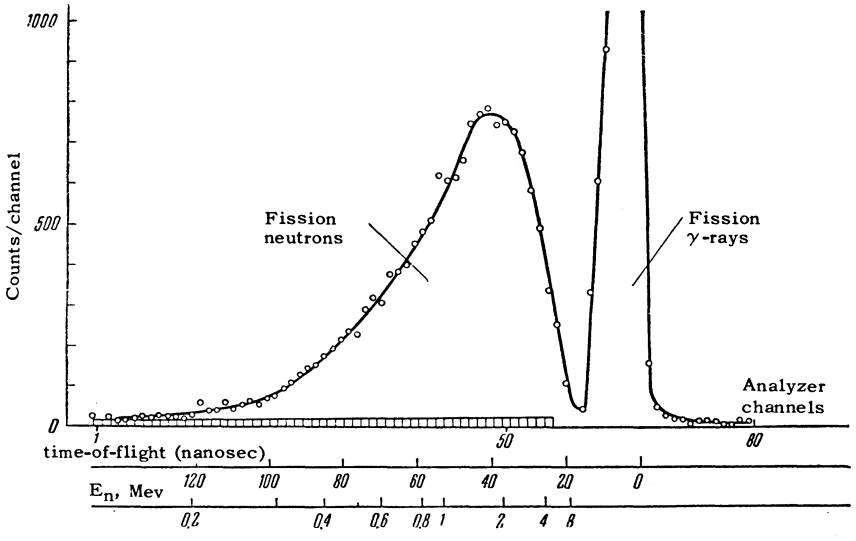

FIG. 6. Time distribution of neutrons and γ rays from U^{238} fission.

time distributions for time-of-flight intervals from 24 to 86 nanosec. The corresponding energy interval was 5 to 0.4 Mev. Data obtained outside this interval were not processed because of the strong background. Measurements for energies less than 0.4 Mev were also unreliable because of possible instability in the efficiency of the detector near the threshold.

The total number of recorded fission neutrons with energies in the 0.4 to 5 Mev interval was 2.2×10^4 for U^{235} and 2.6×10^4 for U^{238}, with the counting rate at 500 — 600 neutrons/hour. The statistical error was 3 — 4% in the 0.8- to 5-Mev interval and rose to 6% in the 0.4- to 0.8-Mev interval. The total error in the measurements may have been increased by inaccuracies in the numerical determination of the energy dependence of the detector efficiency.

To clarify the influence of energy resolution on the form of the fission neutron spectra, control measurements were made of the spectrum of secondary neutrons formed in the passage of 14.3-Mev neutrons through a layer of lead 6-cm thick, with three flight distances: 75, 100, and 125 cm. These measurements showed that as the energy resolution was improved, the form of the spectrum was the same within the limits of accuracy required in the experiments (2%).

III. RESULTS AND DISCUSSION

Figure 7 shows the spectra of neutrons from the fission U^{235} and U^{238} as obtained from the measurements.

To analyze the resultant spectra, $\ln\{F(E)/E\}$ curves (Fig. 8) were plotted.

The hard portion of the spectra ($E > 3$ Mev), due to neutrons emitted by fragments, was used to find the value of parameter T_f (w was assumed to be 0.5 Mev). The difference between the experimental data and Eq. (1) in the region where $E < 3$ Mev determined the spectrum of the neutrons that evaporated before fission. The spectra of fission neutrons from U^{235} and U^{238} were found to be represented by

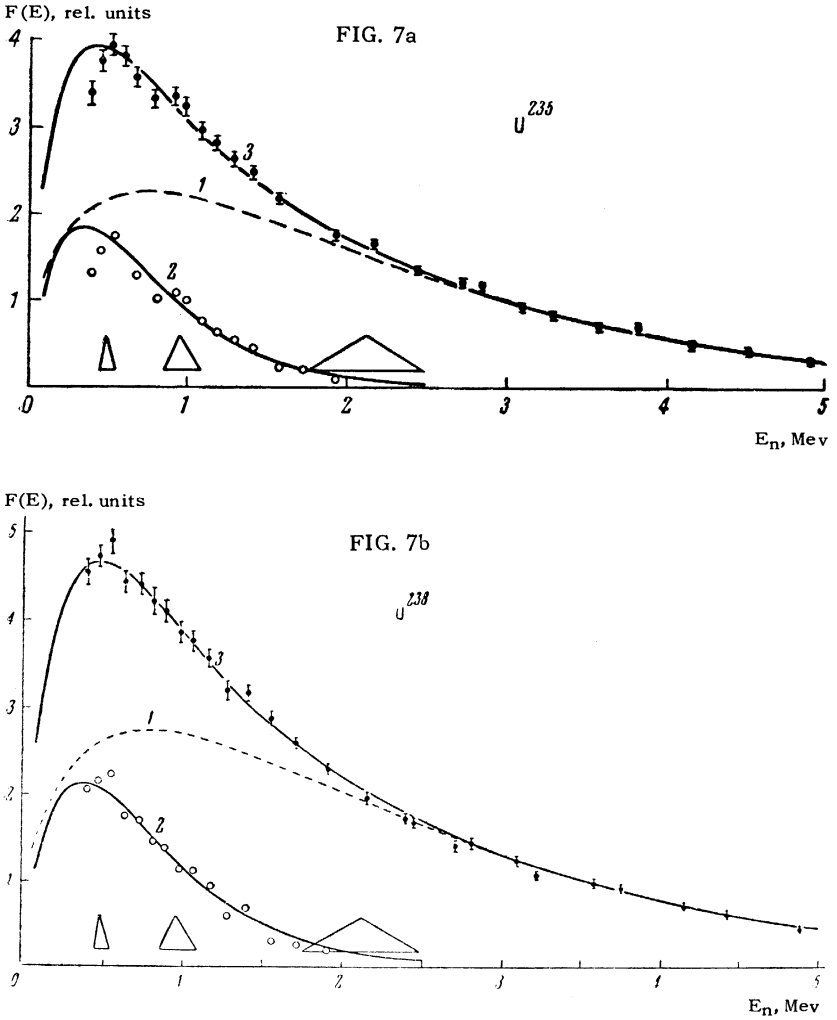

FIG. 7. Neutron spectra obtained from the fission of U^{235} (a) and U^{238} (b): ● — experimental results, o — the result of subtracting curve 1 from the experimental data; curve 1 — distribution given by Eq. (1), 2 — distribution $Ee^{-E/T}$, 3 — sum of curves 1 and 2 (distribution given by Eq. (3)).

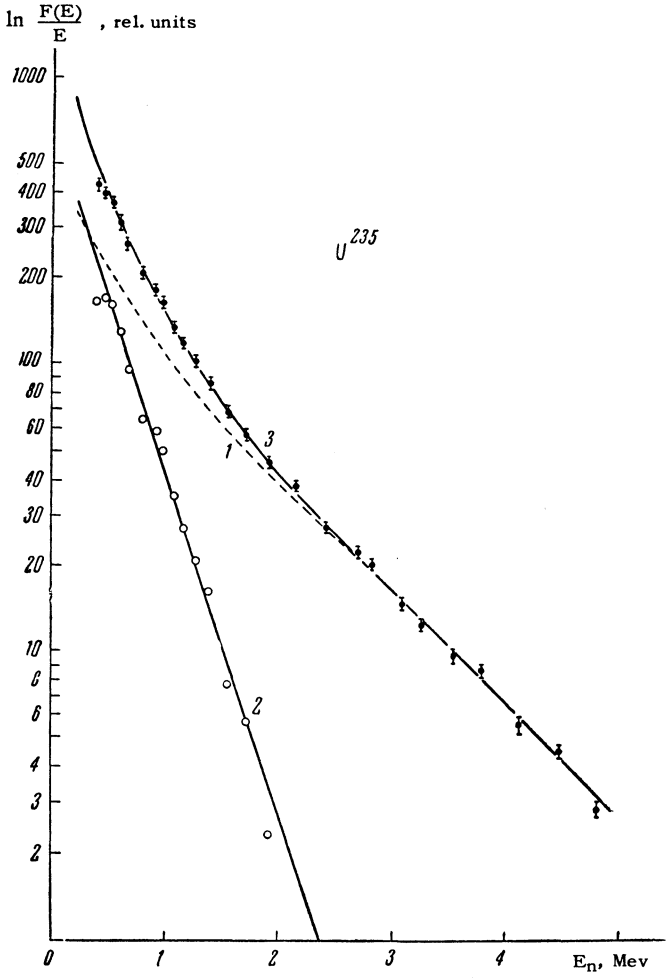

FIG. 8a. Neutron spectra obtained from the fission of U^{235} (designations as in Fig. 7).

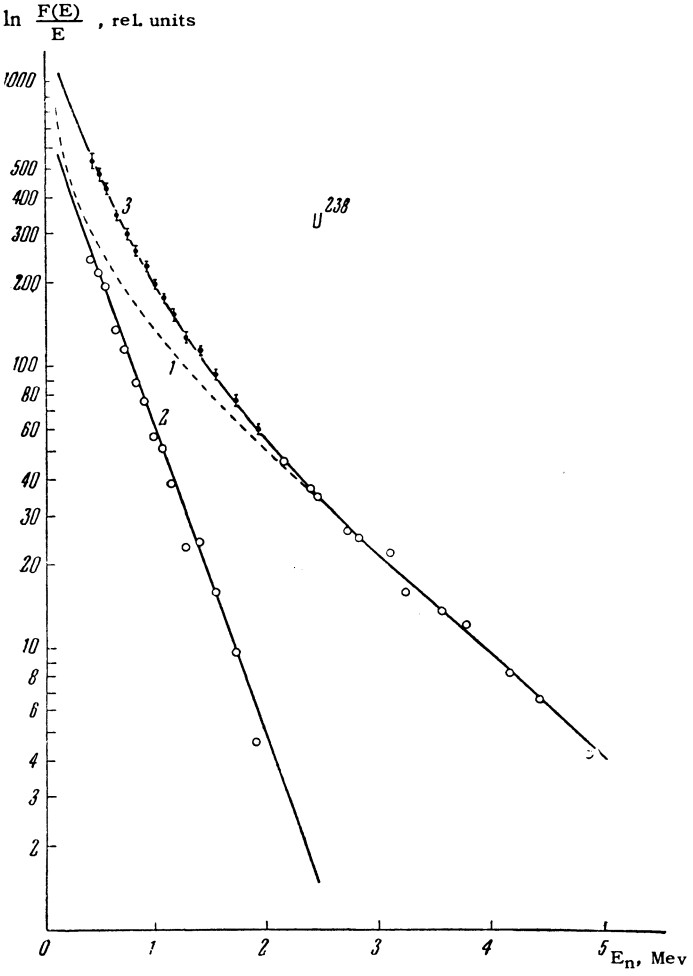

FIG. 8b. Neutron spectra obtained from the fission of U^{238} (designations as in Fig. 7).

$$F(E) = \alpha \frac{E}{T^2} e^{-E/T} + (1-\alpha) \frac{e^{-w/T_f}}{\sqrt{\pi w T_f}} e^{-E/T_f} \sinh \frac{2\sqrt{wE}}{T_f}, \quad (3)$$

with the first term corresponding to neutrons evaporated before nuclear fission and the second corresponding to neutrons emitted by fragments. The values of the parameters are shown in Table I.

So that these results could be compared with data published by other authors, T_f values obtained from nuclear fission induced by thermal, 4-Mev, and 14-Mev neutrons were also included in Table I. Comparison of the T_f values for U^{235} shows that when the neutron energy is increased to 14 Mev, the magnitude of T_f is increased by approximately 10%.

As was noted earlier by Zamyatnin et al.,[7] the neutron spectrum from U^{238} is harder than the spectrum from U^{235}. This finding does not agree with the dependence of T_f on Z^2/A.[18]

To compare our data with the results reported by authors who used Eq. (2) to approximate their fission neutron spectra, values were found for the parameter B. The values for B have been included in Table I and confirm the conclusions reached through comparison of the values of T_f.

As can be seen from Fig. 8, the spectrum of the evaporated neutrons is in good agreement with the $Ee^{-E/T}$ distribution, and the parameter T has nearly the same value for both uranium isotopes. The fraction of evaporated neutrons obtained (about 20%) proved to be considerably greater than expected. If the evaporated neutrons are assumed to occur solely through a (n, nf) reaction with a cross section $\sigma_f' = \sigma_{f_1} - \sigma_{f_0}$, then the yield of evaporated neutrons should be $\alpha = (\sigma_{f_1} - \sigma_{f_0})/\bar{\nu}\sigma_{f_1} \approx 10\%$, where σ_{f_0} and σ_{f_1} are the fission cross sections on the first and second plateaus[19] (see Fig. 9). Allowance for evaporation of neutrons by the (n, 2nf) reaction reduces the divergence somewhat but does not eliminate it, since the cross section for this process is small.[20]

Thus, the measurements indicate a greater probability for (n, nf) and (n, 2nf) processes in the fission of U^{235} and U^{238} by 14-Mev neutrons

TABLE I

Isotope	E_n, Mev	T_f, Mev	B, Mev	T, Mev	α
U^{235}	Thermal	0.965 [2]	1.290 [2,17]	—	—
	4.0	1.01±0.03 **	—	—	—
	14.0	1.05±0.06 [7]	—	0.4±0.05 [7]	—
	14.3	1.06±0.03*	1.36±0.04*	0.37±0.04*	0.16±0.02*
U^{238}	14.0	1.22±0.10 [7]	—	0.48±0.05 [7]	—
	14.3	1.16±0.03*	1.46±0.04*	0.40±0.04*	0.21±0.02*

*Results of the present experiment.

**Obtained on the basis of the relative value given by Bondarenko et al.[16] and the T_f value for thermal neutrons.

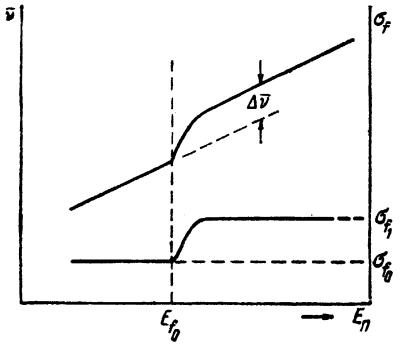

FIG. 9. Proposed $\bar{\nu}(E)$ dependence.

than should result from the values for the fission cross sections on the first and second plateaus and, correspondingly, also indicate a reduction in the probability of nuclear fission without prior neutron evaporation. It is noteworthy that the experimental value of α for U^{238} is somewhat greater than for U^{235} and fits the assumption of a larger contribution by the (n, nf) process to the total fission cross section of U^{238}.

To obtain $\bar{\nu}$, the fission neutron spectra were integrated with allowance for the absolute scintillation-counter efficiency ϵ and the fraction β (≈ 0.15) of the spectrum which was beyond the measured range [β was computed from Eq. (3)]. The result obtained pertained to the fissions that were recorded during the measurement time. A correction was introduced in the calculation of $\bar{\nu}$ to take account of the moderation of the primary neutrons through scattering on the materials in the chamber and target block. The values for $\bar{\nu}$ obtained were 4.17 ± 0.30 for U^{235} and 4.28 ± 0.30 for U^{238}, and their ratio was $\bar{\nu}(U^{238})/\bar{\nu}(U^{235}) = 1.03 \pm 0.03$.

The error in $\bar{\nu}$ consists mostly of errors in determining the values of ϵ and β and on the average amounted to 7 — 8%. The error in the relative measurement was much smaller (~ 3%), since the absolute value of the efficiency was unimportant in this case.

For the sake of comparison, Table II includes values for $\bar{\nu}$ obtained from other investigations

TABLE II

E_n, Mev	$\bar{\nu}(U^{235})$	$\bar{\nu}(U^{238})$
14.0	4.10±0.15 [17]	—
14.1	4.52±0.32 [17]	4.13±0.25 [17]
	4.13±0.24 [11]	4.50±0.32 [11]
		4.45±0.35 [12]
14.2	—	4.55±0.15 [13]
14.8	4.70±0.50 [10]	—
15.0	4.51±0.19 [9]	—
14.3	4.29±0.12*	4.48±0.13*
	4.17±0.30**	4.28±0.30**

*Weighted mean; for reduction to E_n = 14.3 Mev the $d\bar{\nu}/dE_n$ obtained in our work was used.

**Results of this work.

and their weighted mean. The values given in the present article are somewhat lower than the average values for $\bar{\nu}$, though both values for $\bar{\nu}$ and their ratios coincide within the experimental errors.

The absolute values of $\bar{\nu}_{14}$ for fission induced by 14-Mev neutrons taken together with the values of $\bar{\nu}_0$ for thermal neutrons or for low energy neutrons permit one to infer the dependence of $\bar{\nu}$ on the excitation energy E* of the fissionable nucleus (or on the energy, E_n, of the neutrons producing the fission). Moreover, the large change in E_n (to 14 Mev) and correspondingly in $\bar{\nu}$ permits one to find $d\bar{\nu}/dE_n$ with a sufficiently high degree of accuracy.[16] It is usually assumed that

$$d\bar{\nu}/dE_n = (\nu_{14} - \bar{\nu}_0)/(14 - E_0),$$

i.e., $\bar{\nu}$ varies linearly with the energy. Here E_0 is the energy of the low energy or thermal neutrons. The experimental values for $\bar{\nu}$ for excitation energies E* < 10 Mev (E_n < 4 Mev) confirm this assumption.

However, the use of the value of $\bar{\nu}_{14}$ in computing $d\bar{\nu}/dE_n$ is complicated by the fact that when E_n is the same as the fission barrier energy E_f of the original nucleus, a new reaction

channel is opened – (n, nf), and $\bar{\nu}(E)$ may undergo a discontinuity (Fig. 9). The magnitude of the $\Delta\bar{\nu}$ jump at E_f is

$$\Delta\bar{\nu} = \frac{\sigma_f'}{\sigma_{f_1}} [1 - \bar{\nu}(E_f) + \bar{\nu}(E_f - E_b - 2T)],$$

and depends on the contribution σ_f' of the (n, nf) reaction to the total cross section σ_f^f and on the difference $1 - [\bar{\nu}(E_f) - \bar{\nu}(E_f - E_b - 2T)]$ which may have either a positive or negative value. For those cases when the change in $\bar{\nu}$ is equal to unity, i.e., for E_f equal to the sum of the neutron binding energy, E_b, and the average neutron kinetic energy 2T, the discontinuity in $\bar{\nu}(E)$ is absent.*

To evaluate $\Delta\bar{\nu}$, we take for the value of E_b in U^{236} and U^{239}, 6.5 and 4.8 Mev respectively[21] and for the values for $d\bar{\nu}/dE_n$, those given by Bondarenko et al.[16] Thus we find that

$$\bar{\nu}(E_f) - \bar{\nu}(E_f - E_b - 2T) = (E_b + 2T)\, d\bar{\nu}/dE_n$$

is less than unity for both uranium isotopes. A calculation of the value of $\Delta\bar{\nu}$ with allowance for the reduction in $d\bar{\nu}/dE_n$ due to the discontinuity and also with allowance for a second discontinuity in the region of the threshold for the (n, 2nf) reaction indicates that in determining $d\bar{\nu}/dE_n$ it is necessary to reduce the difference $\bar{\nu}_{14} - \bar{\nu}_0$ by 0.10 for U^{235} and 0.16 for U^{238}. The value of $d\bar{\nu}/dE_n$ obtained on the basis of our results in the energy region $E_n < 2$ Mev proved to be 0.112 ± 0.011 for U^{235} and 0.115 ± 0.011 for U^{238}.

From our data we were also able to evaluate the relative yield of prompt fission γ rays. If the spectra of γ rays from the fission of U^{235} and U^{238} are assumed to be alike, then the ratio of the average numbers of γ rays emitted per fission event is $n_\gamma(U^{238})/n_\gamma(U^{235}) = 0.94$.

In conclusion the authors wish to express their gratitude to Yu. Ya. Glazunov, A. N. Maslov, N. I. Nemudrov, V. A. Parshina, A. I. Peshetov, V. S. Khorkhordin, and V. N. Shikin, who participated in the measurements, to the crew of radio technicians for setting up the electronic apparatus, to V. A. Komarova for her work on the computer, and also to the associates in V. A. Ivanov's group for seeing to the operation of the accelerator.

*In this case $\bar{\nu}$ is considered to be the same for neighboring isotopes.

[1] B. E. Watt, Phys. Rev. **87**, 1037 (1952); Bonner, Ferrell, and Rinehart, Phys. Rev. **87**, 1032 (1952); D. L. Hill, Phys. Rev. **87**, 1034 (1952); Mukhin, Barkov, and Gerasimova, see B. G. Erozolimskiĭ, Атомная энергия (Atomic Energy) Supplement No. 1, p. 74 (1957); [Transl: The Physics of Fission, Consultants Bureau, Inc., New York, 1957, p. 51].

[2] Cranberg, Frye, Nereson, and Rosen, Phys. Rev. **103**, 662 (1956).

[3] J. A. Grundl and J. R. Neuer, Bull. Amer. Phys. Soc. Series II **1**, 95 (1956).

[4] Kovalev, Andreev, Nikolaev, and Guseĭnov, JETP **33**, 1069 (1957), Soviet Phys. JETP **6**, 825 (1958).

[5] V. P. Kovalev, JETP **34**, 501 (1958), Soviet Phys. JETP **7**, 345 (1958).

[6] Smith, Fields, Friedman, Cox, and Sjoblom, Paper No. 690, Second International Conference on the Peaceful Uses of Atomic Energy (Geneva, 1958), Vol. 15, p. 392.

[7] Zamyatnin, Safina, Gutnikova, and Ivanova, Атомная энергия (Atomic Energy) **4**, 337 (1958); Soviet Journal of Atomic Energy (Eng. Transl.) **4**, 443 (1958).

[8] G. A. Bat' and L. P. Kudrin, ibid. **3**, 15 (1957); Soviet Journal of Atomic Energy (English Translation) **3**, 735 (1957).

[9] Smirenkin, Bondarenko, Kutsaeva, Mishchenko Prokhoronova, and Shemetenko, ibid. **4**, 188 (1958); Soviet Journal of Atomic Energy (Eng. Transl.) **4**, 253 (1959).

[10] A. N. Protopopov and M. V. Blinov, ibid. **4**, 374 (1958); Soviet Journal of Atomic Energy (Eng. Transl.) **4**, 491 (1958).

[11] N. N. Flerov and V. M. Talyzin, ibid. **5**, 653 (1958); Soviet Journal of Atomic Energy (Eng. Transl.) **5**, 1593 (1958).

[12] N. N. Flerov and E. A. Tamanov, ibid. **5**, 654 (1958); Soviet Journal of Atomic Energy (Eng. Transl.) **5**, 1596 (1958).

[13] M. Gandin and J. L. Leroy, Paper No. 1186, Second International Conference on the Peaceful Uses of Atomic Energy (Geneva, 1958).

[14] J. E. Hardy, Rev. Sci. Instr. **29**, 705 (1958).

[15] Maienschein, Peele, Zobel, and Love, loc. cit. ref. 6, Paper No. 670, Vol. 15, p. 366

[16] Bondarenko, Kuz'minov, Kutsaeva, Prokhorova, and Smirenkin, ibid. Paper No. 2187, Vol. 15, p. 353.

[17] R. B. Leachman, ibid. Paper No. 2467, Vol. 15, p. 229.

[18] V. P. Kovalev and V. S. Stavinskiĭ, Атомная энергия (Atomic Energy) **5**, 649 (1958); Soviet Journal of Atomic Energy (Engl. Transl.) **5**, 1588 (1958).

[19] Yu. S. Zamyatnin, ibid., Supplement No. 1 p. 27 (1957); [Transl: The Physics of Fission, Consultants Bureau, Inc., New York, 1957].

[20] D. J. Hughes and R. B. Schwartz, Neutron Cross Sections, BNL-325, New York 1958.

[21] R. Vandenbosch and G. T. Seaborg, Phys. Rev. **110**, 507 (1958).

Translated by A. Skumanich
138